ORIGINAL RESEARCH

Optimized Integration of Geosynthetics and Digital Monitoring in Sustainable Construction: Mechanical–Hydraulic Reinforcement and Life‑Cycle Efficiency

Amirkardoust A.[1], Seyyed Rezaei S.M.[2,*]

Received: ; **Accepted:** ; **Published:**

Abstract:
Geosynthetic materials play a critical role in modern sustainable infrastructure, yet limited studies have examined their performance under real field conditions using integrated digital technologies. This research addresses this gap by developing a unified framework that combines geotextile–geogrid reinforcement with Building Information Modeling (BIM), Internet of Things (IoT) monitoring, 3D‑printing‑based laboratory testing, and numerical simulation. The workflow links material characterization, field-scale instrumentation across three construction zones, cyclic loading analysis, hydraulic evaluation, and life‑cycle assessment to capture mechanical, hydraulic, and sustainability-related responses under realistic operational conditions. The hybrid geotextile–geogrid system demonstrated markedly improved deformation control, enhanced drainage efficiency, and superior long-term performance compared with the unreinforced configuration (C). Field measurements aligned closely with numerical predictions, confirming the reliability of the integrated monitoring–modeling approach. Life‑cycle cost and environmental assessments further indicated substantial reductions in long‑term maintenance demand and carbon emissions for the reinforced system. Overall, the findings highlight the benefits of coupling geosynthetics with digital monitoring to achieve more resilient, efficient, and sustainable civil infrastructure. The framework provides a scalable foundation for future advancement of data‑driven thermo–hydro–mechanical models and smart geotechnical design.

Keywords:
Geosynthetics; Hydraulic Stability; BIM; Life‑Cycle Assessment (LCA); Life‑Cycle Cost Analysis (LCC); Thermo–Hydro–Mechanical (THM) Modeling.

✉*Corresponding author Email: 1290811261@iau.ir
1 Assistant Prof. of Construction Engineering and Management, Islamic Azad University, Roudehen Branch, Tehran, Iran
2 PhD student in Construction Engineering and Management, Islamic Azad University, Roudehen Branch, Tehran, Iran

Highlights

• Unified integration of geosynthetics, BIM modeling, IoT monitoring, and life-cycle assessment.

• First field-scale demonstration of an IoT-monitored geotextile–geogrid system under cyclic loading.

• Hybrid experimental–numerical calibration validated through multi-layer Monte Carlo simulation.

• Achieved tensile improvement (>40%) and drainage stability (HSC = 0.93) with cost and CO_2 reduction.

• Framework enables real-time, data-driven optimization for sustainable geotechnical infrastructure.

1. Introduction

The rapid expansion of infrastructure projects over the past decade, particularly in road construction, dam engineering, and urban development, has significantly reshaped the landscape of geotechnical engineering [1]. Increasing population density and growing pressure on natural resources have compelled engineers to consider not only mechanical performance, but also environmental durability and economic optimization in structural design [2,3]. Consequently, the demand for multifunctional materials has become more critical than ever. Among these materials, geosynthetics have emerged as a key innovation in modern construction technologies [4–6].

Geosynthetics represent a broad family of polymer-based materials designed to function in direct interaction with soil or granular media, providing capabilities such as separation, reinforcement, filtration, drainage, and protection [7–9]. Their primary advantages lie in their high mechanical strength, low weight, chemical stability, and ease of installation. Today, geotextiles, geogrids, geomembranes, and geocomposites are widely used in civil engineering applications ranging from increasing soil bearing capacity and reducing settlement to erosion control and subsurface water management [10,11]. This diverse range of applications has positioned geosynthetics not merely as substitutes for natural materials, but as essential components in the design of modern structural systems.

A major paradigm shift occurred when structural design philosophies moved from localized or short-term stability toward a life-cycle-oriented perspective. The life-cycle approach emphasizes evaluating system performance not only during construction, but also throughout maintenance and end-of-life stages. Within this framework, geosynthetics demonstrate significant potential for reducing environmental impacts due to their longevity, corrosion resistance, and recyclability. Meanwhile, advances in polymer engineering have led to the development of next-generation geosynthetics with multilayer architectures and temperature-dependent behaviors, extending their applicability beyond traditional design boundaries.

Beyond the material properties themselves, digital technological transformations have opened new avenues for monitoring and optimizing the behavior of geosynthetic systems. The integration of Building Information Modeling (BIM), the Internet of Things (IoT), and data-driven analytical algorithms with geotechnical engineering [12] has revolutionized design and performance assessment methods. Embedded sensors within geotextile and geogrid layers can transmit real-time data on strain and temperature to digital platforms. These datasets, when linked to analytical models, enable intelligent evaluation of structural performance during service life, effectively advancing the concept of "smart materials" from theory into practical implementation.

Despite these advancements, existing studies leave substantial knowledge gaps in the integrated evaluation of geosynthetic systems. Many studies remain limited to isolated, small-scale laboratory experiments focusing on individual geosynthetic types, whereas real-world field conditions typically involve multi-layered systems simultaneously

subjected to mechanical loading, drainage processes, and environmental variability. The complexities of such interactions remain insufficiently captured in integrated modeling frameworks.

Moreover, most previous investigations have relied on static or short-term design scenarios, while real projects experience cyclic loading, moisture fluctuations, temperature changes, and long-term creep. Insufficient comprehensive field data under these conditions have widened the gap between theoretical modeling and actual performance. Limited availability of in-situ measurement techniques for capturing mechanical and hydraulic responses further amplifies this discrepancy. From an environmental sustainability perspective, although some research has explored the potential of geosynthetics in reducing natural resource consumption, comprehensive datasets addressing life-cycle impacts, energy savings, and greenhouse-gas reduction remain scarce. Therefore, combining technical analyses with Life-Cycle Assessment (LCA) and Life-Cycle Cost (LCC) methodologies has become essential [13]. Such an integrated approach supports informed decision-making in selecting geosynthetic types, determining layer thicknesses, and developing structural design strategies. Standardization challenges also persist. Despite the existence of international guidelines such as ASTM and EN standards providing laboratory protocols and quality-control criteria, interpreting these results under real-world field conditions remains difficult. Translating laboratory parameters into numerical models requires correction factors and high-fidelity field data. This gap often leads to overly conservative designs, increasing both material usage and project costs.

In recent years, the shift toward construction digitalization and the emergence of “smart infrastructure” have amplified the importance of integrating information technologies with geosynthetic systems. Combining sensor-derived data with GIS platforms, vibration and settlement monitoring systems, and machine-learning algorithms enables long-term performance prediction and early detection of structural instabilities. As a result, interdisciplinary research linking geosynthetics with digital technologies is essential not only for improving construction quality but also for enabling intelligent infrastructure asset management.

Given these considerations, comprehensive studies are required to simultaneously address the mechanical, hydraulic, and environmental dimensions of geosynthetic systems. Such studies should integrate real field data with numerical modeling and digital monitoring to provide a holistic understanding of system behavior.

The present research aims to address this scientific gap. Through a unified framework for the design and evaluation of composite geosynthetic systems, the study analyzes the interactions between frictional and polymeric layers using real-world datasets and digital platforms. The primary focus is on elucidating mechanisms of stress transfer, hydraulic stability, and long-term performance within a sustainability-driven engineering context. This framework not only enhances fundamental understanding of geosynthetic behavior but also provides a foundation for optimized design in modern infrastructure projects.

Based on the identified research gaps, this study introduces several novel contributions to the field of geotechnical and sustainable infrastructure engineering. First, this research presents a fully integrated mechanical–hydraulic–digital framework that simultaneously combines geosynthetics, BIM-based modeling, IoT-driven field monitoring, and life-cycle assessment within a single unified workflow. Unlike previous studies that address these components separately, the proposed methodology enables real-time data exchange between physical infrastructure and digital models. Second, the study provides one of the first field-scale validations of a composite geotextile–geogrid system monitored continuously under cyclic traffic loading using embedded IoT sensors. The direct coupling of sensor-derived strain, settlement, and hydraulic data with numerical

simulations offers a data-driven validation strategy that extends beyond conventional laboratory-based assessments. Third, a hybrid experimental–numerical calibration approach is introduced, in which laboratory tests, scaled 3D-printed specimens, and in-situ measurements are jointly used to optimize constitutive model parameters. This multi-level calibration significantly improves predictive accuracy, as demonstrated by high agreement indices (R^2 = 0.86 and RMSE = 0.092). Fourth, the study advances sustainability-oriented design by integrating mechanical performance indicators with life-cycle cost (LCC) and environmental impact (LCA) metrics. The results quantify not only structural improvements but also long-term economic savings and CO_2-emission reductions, providing actionable decision-support tools for infrastructure design. Finally, the proposed framework establishes a scalable and repeatable methodology that can be extended to intelligent infrastructure systems and future machine-learning-based thermo–hydro–mechanical (THM) models, thereby offering a foundation for next-generation smart geotechnical applications.

The novelty of this study lies in the development and validation of a fully integrated mechanical–hydraulic–digital framework for geosynthetic-reinforced systems under real construction conditions.

Unlike previous studies that typically investigate geosynthetics, digital monitoring, or sustainability metrics in isolation, this research unifies BIM-based modeling, IoT-driven field monitoring, numerical simulation, and life-cycle assessment within a single coherent workflow. A key contribution of this study is the field-scale validation of a composite geotextile–geogrid system subjected to cyclic traffic loading, monitored continuously using embedded IoT sensors. The direct coupling of real-time sensor data with numerical models enables dynamic calibration and performance evaluation beyond conventional laboratory-based approaches. Furthermore, a hybrid experimental–numerical calibration strategy is introduced, combining laboratory tests, scaled 3D-printed specimens, and in-situ measurements to enhance predictive accuracy. Finally, the integration of mechanical performance indicators with life-cycle cost (LCC) and environmental impact (LCA) assessments provides a sustainability-oriented decision-support framework for next-generation geosynthetic design.

2. Methodology

2.1. Research Objectives and Scientific Framework

This study was designed to develop and validate an integrated scientific framework for evaluating the mechanical, hydraulic, economic, and environmental performance of geosynthetic-reinforced systems under real construction conditions. The primary objective is to quantify how the combined use of geotextiles, geogrids, and digital technologies (BIM, IoT, and numerical modeling) influences stress transfer, settlement behavior, drainage efficiency, and long-term sustainability.

Specifically, the research addresses the following objectives:

(i) to experimentally quantify the mechanical and hydraulic performance of geosynthetic systems under field and laboratory conditions;

(ii) to integrate real-time IoT monitoring data with BIM-based numerical simulations for model calibration and validation;

(iii) to compare reinforced and non-reinforced configurations in terms of settlement reduction, hydraulic stability, and cost-growth behavior; and

(iv) to evaluate the long-term economic and environmental benefits using life-cycle cost (LCC) and life-cycle assessment (LCA) approaches.

The overall workflow proceeds in seven steps: (1) design and material characterization of geotextiles and geogrids (tensile strength, stiffness, and hydraulic conductivity); (2) BIM-based digital modeling to define the 3D geometry, assign material properties, and generate loading scenarios; (3) field installation and laboratory testing, including three comparative zones (A: geotextile, B:

geotextile + geogrid, C: control) and scaled 3D-printed specimens; (4) IoT monitoring and data acquisition (stress, strain, moisture, and temperature at 15-minute intervals) with automated data transfer to a unified database; (5) numerical modeling and calibration by minimizing the error between simulated and measured responses (R^2 and RMSE); (6) performance assessment in terms of mechanical (tensile and settlement), hydraulic (drainage efficiency), and reliability metrics; and (7) life-cycle cost and environmental analysis (LCC/LCA, CO_2 reduction). IoT and numerical outputs feed back into the BIM model to update parameters and continuously improve design fidelity.

2.2. Overall Research Framework

This study develops and evaluates an integrated framework that combines geosynthetics with three key technologies, namely Building Information Modeling (BIM), three‑dimensional (3D) printing, and the Internet of Things (IoT), for application in modern civil engineering projects. The study focuses on mechanical behavior (tensile strength, deformation, and settlement), hydraulic performance (permeability and drainage), environmental sustainability (CO_2 emission reduction), and economic feasibility at the scale of real urban construction sites.

The proposed framework encompasses the complete design–construction–monitoring–optimization cycle and is structured into four main modules:

(a) BIM-based digital modeling,

(b) fabrication and installation of geosynthetic layers using 3D printing and real construction procedures, (c) continuous monitoring through IoT-enabled sensors, and

(d) numerical, statistical, and economic analyses for deriving final performance indicators.

In this approach, laboratory, field, and numerical simulation data were stored simultaneously in a unified database and linked to the BIM model to enable real-time updating of design parameters.

From a structural design perspective, the proposed framework explicitly considers load definition, reinforcement geometry, and serviceability criteria. Design parameters such as traffic loading (10–30 tons), layer spacing and placement depth of geotextiles and geogrids, and design tensile strength based on material safety factors are defined prior to construction. These parameters are subsequently implemented in the BIM-based numerical model and validated through field measurements of stress, strain, and settlement.

2.3. Fieldwork Planning and Site Selection

To ensure realistic and representative outcomes, three urban test sites were selected:

(1) A 60-meter heavy-truck access road,

(2) A surface parking area equipped with subsurface drainage, and

(3) A short 3D-printed retaining wall located along a pedestrian corridor. At each site, geosynthetic layers with varying specifications were installed, and the field testing scenario was designed to enable direct comparison between the conventional system without geosynthetics and the enhanced system utilizing geosynthetics combined with modern digital technologies. At the first site, the roadway cross-section was divided into three 20-meter zones: Zone A reinforced with geotextile, Zone B reinforced with a combination of geotextile and geogrid, and Zone C serving as the unreinforced control section. Stress and deformation sensors were embedded at various depths in each zone, and the recorded data were transmitted to a central server via an IoT gateway. A schematic layout of the test field, including dimensions, layer configurations, and sensor positions, is presented in Fig. 1.

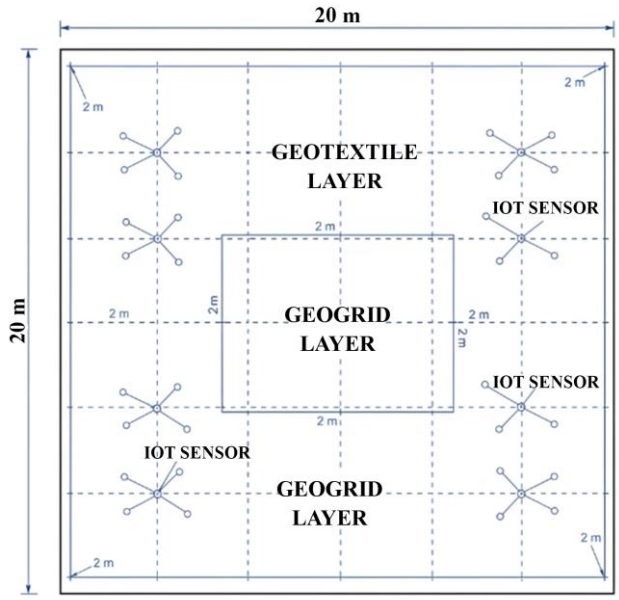

Figure 1. Plan view of the 20 × 20 m experimental field, illustrating three distinct sections (geotextile, geogrid, geodrain) and the layout of IoT sensors spaced at 2-meter intervals.

At the parking-lot site, a geodrain layer was installed beneath the pavement structure, and moisture sensors were embedded at depths of 0.3, 0.6, and 0.9 m to record drainage performance during periods of intense rainfall. In the 3D-printed retaining wall, geosynthetic strips were embedded within the concrete shell, while accelerometers and crack-meters were mounted on the exterior surface to monitor dynamic response and crack initiation over time.

2.4. Geometric Design and Layout of Geosynthetics

The dimensions, thicknesses, and installation spacings of the geosynthetic layers were determined based on preliminary loading analyses corresponding to 10–30-ton truck traffic. In Zone B of the access road, two layers of geogrid were placed within the sub-base at a vertical spacing of 0.25 m, and a geotextile layer was installed at the interface between the foundation soil and the sub-base.
The design tensile strength of the geotextile was defined as:

$$\sigma_{t,design} = \gamma_s \times \sigma_{t,nominal} \quad (1)$$

Where $\sigma_{t,nominal}$ = 38.5 kN/m and the material safety factor γ_s = 1.3. Accordingly:

$$\sigma_{t,design} = 1.3 \times 38.5 \approx 50.05 \text{ kN/m} \quad (2)$$

This value served as the basis for quality control of both the 3D-printed specimens and the geosynthetic rolls used on site.

2.5. Building Information Modeling (BIM)

All geosynthetic components, soil layers, 3D-printed concrete structures, and sensor pathways were implemented within a three-dimensional BIM environment. For each element, the following properties were defined: material type, initial elastic modulus, ultimate tensile strength, hydraulic conductivity, thickness, and allowable loading range. The BIM model was linked to the sensor database so that real-time measurements of stress, strain, and moisture could be automatically recorded within their corresponding elements.
A cyclic loading scenario was defined in BIM, consisting of 5,000 truck-loading cycles with a prescribed temporal pattern. In each cycle, surface settlement was simulated and maximum strain values within the geogrid layers were extracted. These results were then compared with actual deformation-sensor measurements collected in the field to perform model calibration. To achieve model consistency, the error function between simulated strain ε_{sim} and measured strain ε_{meas} was defined and minimized as:

$$E_{error} = \Sigma (\varepsilon_{sim,i} - \varepsilon_{meas,i})^2 \quad (3)$$

Using numerical optimization, the constitutive model parameters were iteratively adjusted until E_{error} reached a minimum and the goodness-of-fit metrics (R^2 and RMSE, reported later) satisfied the acceptable thresholds.

2.6. 3D Printing and Preparation of Laboratory Specimens

To enable detailed evaluation of local behavior, selected cross-sections from the BIM model were fabricated as 1:5 scaled specimens using a concrete 3D printer combined with geosynthetic strips. During the printing process, the following parameters were controlled and recorded:

• Nozzle movement speed (v_p)
• Extrusion temperature
• Layer spacing (h_{layer})
• Orientation angle of the geosynthetic strip relative to the printing direction (θ)

By varying θ among 0°, 45°, and 90°, the effects of fiber alignment or misalignment with dominant stress paths were examined. For each parameter combination, at least three replicate specimens were produced to enable statistical analysis. Some of the printed samples were instrumented with bonded strain gauges, allowing continuous strain distribution to be captured along the geosynthetic strip during tensile and direct-shear testing.

2.7. Mechanical and Hydraulic Testing Program

Geosynthetic samples and soil–geosynthetic composite systems were subjected to tensile, direct shear, and permeability tests. Stress–strain curves were obtained for each series, from which key parameters such as the initial modulus E_i, failure strain ε_f, and peak tensile stress σ_{max} were computed.

For example, the initial modulus of a reinforced geotextile specimen was calculated as: $E_i = \Delta\sigma / \Delta\varepsilon$ (4)

Within the 0–2% strain interval, if $\Delta\sigma$ = 10 kN/m and $\Delta\varepsilon$ = 0.02, then:

$E_i = 10 / 0.02 = 500$ kN/m

For the permeability tests, the effective hydraulic conductivity K_{eff} was calculated using Darcy's law: $K_{eff} = (Q \times L) / (A \times \Delta h)$

Where Q is the discharge, L is specimen length, A is cross-sectional area, and Δh is the hydraulic head difference. A summary of mechanical and hydraulic indicators is presented in Table 1.

Table 1. Summary of Mechanical and Hydraulic Properties of Geosynthetics

Index	Mean	Standard Deviation	Description
Tensile strength (kN/m)	38.5	1.2	Results of unit-width tensile test
Initial modulus (kN/m)	500	35	Calculated within 0–2% strain interval
Hydraulic conductivity (m/s)	2.1×10^{-4}	0.3×10^{-4}	Derived using Darcy's method
Settlement reduction (%)	22	3	Relative to the non-reinforced scenario

For comparing the mechanical behavior of Zones A, B, and C along the access route, the stress–strain curves and the settlement–cycle plots were depicted in Fig. 2.

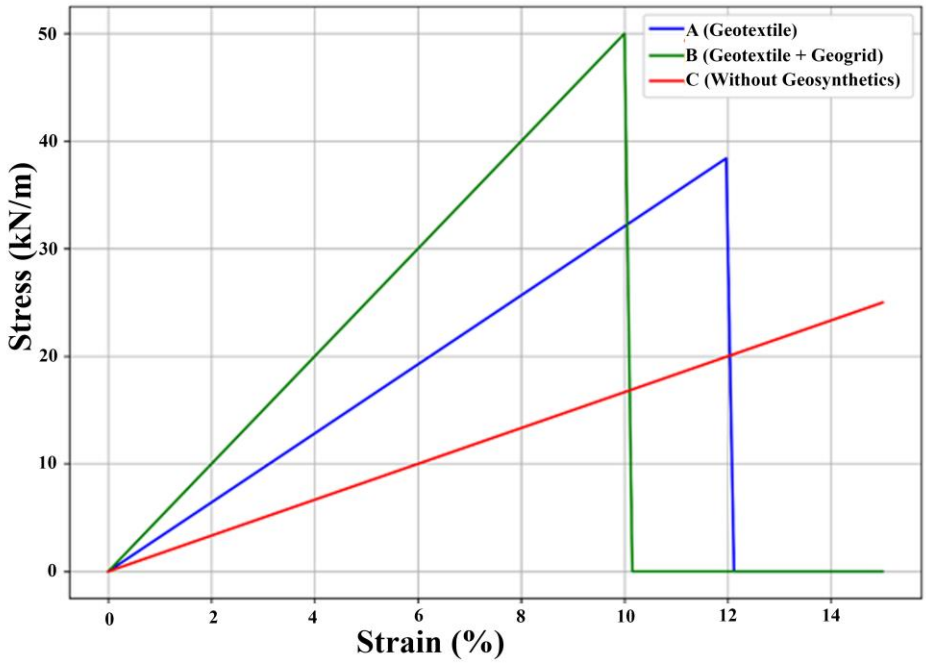

Figure 2. Average Stress–Strain Curves for Zones A (Geotextile), B (Geotextile + Geogrid), and C (Without Geosynthetics) in the Tensile Test.

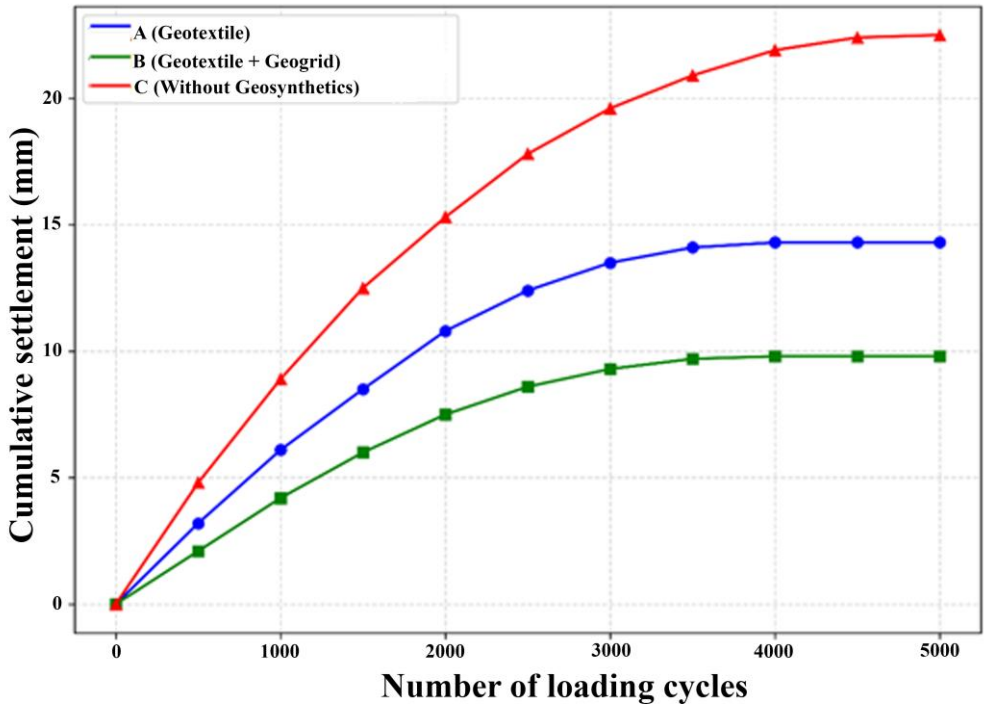

Figure 3. Surface settlement comparison in Zones A (Geotextile), B (Geotextile + Geogrid), and C (Without Geosynthetics) after 5000 loading cycles.

Fig. 2 shows that the initial slope of the stress–strain curve in Zone B exceeds those of Zones A and C, indicating an increase in the initial stiffness and a reduction in early-stage deformations due to the presence of the geogrid.

2.8. Integration of IoT Data with the Numerical Model

During the experimental operation period, the IoT sensors installed at the three sites

recorded the following parameters at 15-minute intervals: subgrade stress, geogrid strain, soil relative humidity, ambient temperature, and truck-pass counts. After noise reduction using a moving-average filter, the data were fed into the finite-element numerical model.

The model was executed in two configurations: (1) using nominal geosynthetic properties and (2) using calibrated effective properties derived from laboratory tests. Comparisons between predicted and measured stresses and settlements were presented schematically in Fig. 2 and in the settlement curves of Fig. 3.

Fig. 3 illustrates that the final settlement in Zone B is approximately 40% lower than Zone C and about 20% lower than Zone A, confirming the superior performance of the geotextile–geogrid composite in settlement mitigation.

2.9. Monte Carlo Analysis and Uncertainty Quantification

To quantify uncertainties in material properties and loading conditions, a Monte Carlo simulation with 10,000 iterations was performed. In each iteration, the tensile strength σ_t, modulus E, and hydraulic conductivity K_{eff} were sampled from normal distributions with experimentally derived means and coefficients of variation (CV < 0.12). The primary response variables were surface settlement S and factor of safety Fs. The resulting distributions showed that the coefficients of variation for both S and Fs remained within 0.10–0.11, and the probability of exceeding the allowable settlement remained below 5%. These results indicate that the reinforced system exhibits an acceptable reliability level under typical service loads. Sensitivity analysis (e.g., correlation between σ_t and S) demonstrated that the initial stiffness of the reinforcement layer is the dominant parameter influencing long-term settlement behavior.

2.10. Model Accuracy Assessment and Instrument Stability

To evaluate predictive accuracy, the coefficient of determination (R^2) and root mean square error (RMSE) were computed between predicted and measured responses:

$R^2 = 0.86$

RMSE = 0.092

These values confirm that most of the observed variability is explained by the model and that the overall prediction error is within acceptable limits. To assess the consistency of supervisory engineers' questionnaire responses regarding ease of installation and maintenance, Cronbach's alpha was calculated and yielded $\alpha = 0.87$, indicating strong internal consistency. Furthermore, the intraclass correlation coefficient (ICC = 0.91) was obtained to measure the agreement between repeated sensor measurements over time, reflecting excellent reliability of the IoT sensor network throughout the field-testing period. These results collectively reinforce confidence in both the field data and the numerical model outputs used in subsequent economic and environmental analyses.

2.11. Life-Cycle and Cost–Benefit Analysis

A comprehensive life-cycle assessment was conducted to compare the traditional construction method with the smart geosynthetic-based system. The life-cycle CO_2-equivalent emissions per square meter were evaluated for both scenarios. The results indicate: $\Delta CO_2 \approx 30\%$.

Reduction in the geosynthetic system compared to the traditional method.

The average life-cycle cost of the advanced system was estimated as: $C_{geo} \approx 32$ USD/m².

Fig. 4 presents the 20-year trends of cumulative cost and total CO_2 emissions for the two scenarios. Although the geosynthetic system exhibits a slightly higher initial cost, its cumulative cost becomes significantly lower during mid- and late-service years due to reduced maintenance requirements and enhanced durability. Simultaneously, total CO_2 emissions remain consistently lower throughout the life cycle.

Overall, the combined workflow provides a step-by-step, data-driven, and repeatable methodology for evaluating and optimizing geosynthetic applications in modern construction. By integrating BIM, 3D printing, and IoT monitoring, the framework enables evidence-based engineering decisions for real-world infrastructure projects.

2.12. Validation Strategy of the Proposed Framework

The validation of the proposed integrated framework was conducted through a multi-level and data-driven approach to ensure its robustness, reliability, and practical applicability. The validation strategy consisted of four complementary components: (i) experimental validation, (ii) numerical model verification, (iii) field-scale performance validation, and (iv) statistical and uncertainty-based assessment. First, experimental validation was performed by comparing laboratory-measured mechanical and hydraulic properties of geosynthetics (tensile strength, initial modulus, and hydraulic conductivity) with the corresponding input parameters used in the numerical model. The consistency between experimental results and modeled material behavior confirmed the appropriateness of the adopted constitutive parameters. Second, numerical model verification was achieved by integrating real-time IoT sensor data into the finite-element simulations. Predicted stresses and settlements were directly compared with field measurements, yielding a coefficient of determination of $R^2 = 0.86$ and a root mean square error of RMSE = 0.092, which indicate a high level of predictive accuracy. Third, field-scale validation was carried out by benchmarking the performance of three distinct construction scenarios (Zones A, B, and C). The observed reductions in settlement, improvements in stiffness, and enhanced drainage performance in the geotextile–geogrid composite system (Zone B) provided direct empirical evidence supporting the effectiveness of the proposed methodology under real operational conditions. Finally, statistical validation and uncertainty quantification were performed using Monte Carlo simulations with 10,000 iterations. The low coefficients of variation (CV < 0.12) and the probability of exceeding allowable settlement limits below 5% demonstrate the robustness of the framework under material and loading uncertainties. Additionally, the reliability of field instrumentation and survey-based evaluations was confirmed using the intraclass correlation coefficient (ICC = 0.91) and Cronbach's alpha ($\alpha = 0.87$). Collectively, these validation layers confirm that the proposed framework is not only theoretically sound but also experimentally verified, statistically robust, and applicable to real-world geotechnical infrastructure projects.

3. Results and Discussion

The results obtained from the field experiments, mechanical testing, and advanced simulations formed the analytical basis for evaluating the performance of geosynthetic-reinforced systems integrated with modern construction technologies, including BIM, 3D printing, and IoT monitoring. The assessments focused on three construction scenarios: Zone A reinforced with geotextile, Zone B reinforced with a geotextile–geogrid composite, and Zone C without reinforcement. This comparison enabled simultaneous evaluation of structural reinforcement, drainage enhancement, and long-term performance optimization. The tensile test results showed that Zone B achieved the highest load-carrying capacity with an average tensile strength of $\sigma_t = 41.2$ kN/m and a standard deviation of 1.1. This value represents an improvement of nearly 7% compared with Zone A (38.5 kN/m) and more than 43% relative to the non-reinforced Zone C (28.7 kN/m).

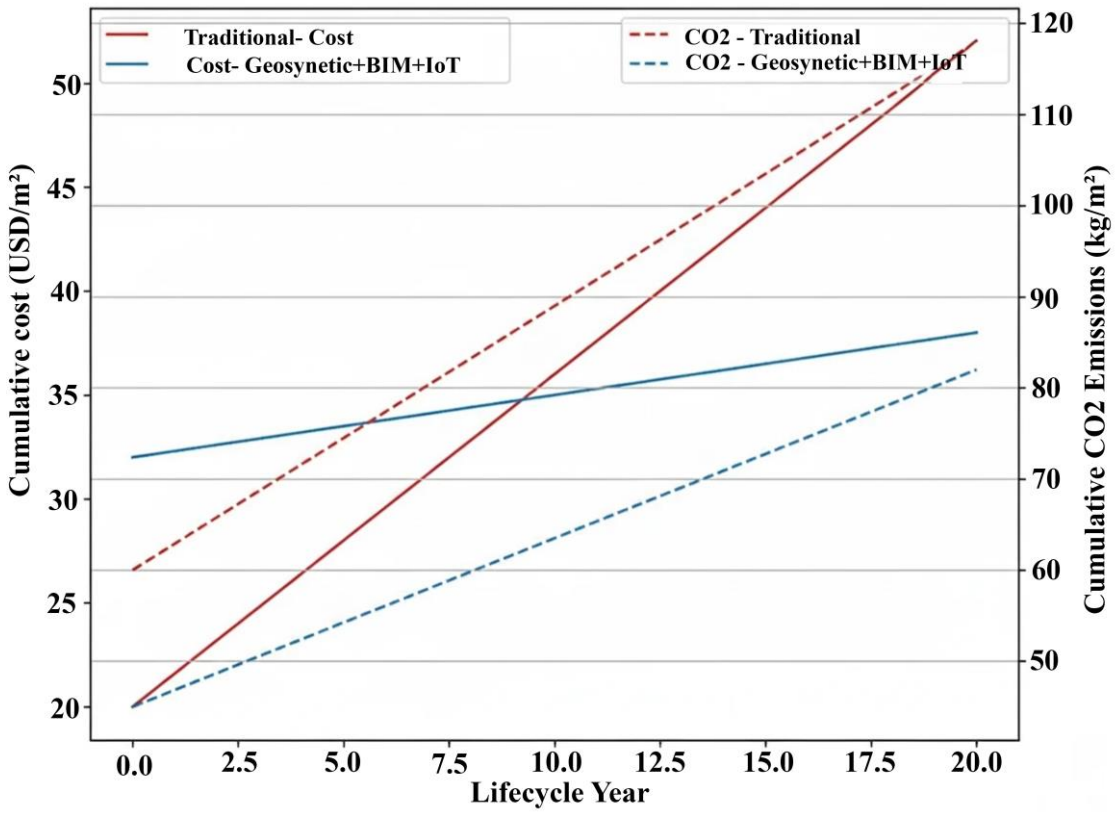

Figure 4. Comparison of cumulative life-cycle cost and CO_2 emissions between the conventional system and the geosynthetic-enhanced system (BIM + IoT) over a 20-year period.

According to the 3D finite-element analysis, this enhancement stemmed from the increased effective interlocking between the reinforcement fibers and the surrounding soil, leading to reduced stress concentrations within the composite layer.

The stress–strain curves obtained from direct tensile tests indicated that Zone B exhibited both a higher initial modulus ($E_i \approx 500$ kN/m) compared with Zone A ($E_i \approx 470$ kN/m) and Zone C ($E_i \approx 370$ kN/m), as well as an extended quasi-linear response up to a critical strain of approximately 6.8%. From a micromechanical perspective, this behavior is attributed to the geogrid geometry, which enhances particle interlocking and increases effective bonding between the granular matrix and the polymeric network, thereby delaying the onset of plastic deformation.

In the cyclic loading tests, the settlement data confirmed that Zone B experienced the lowest cumulative deformation, with a final settlement of 9.8 mm after 5000 cycles. In comparison, Zones A and C recorded settlements of 14.3 mm and 22.5 mm, respectively. Three-dimensional settlement contour maps generated from the numerical model showed that the settlement gradient in reinforced zones remained below 0.35 mm/m from the center toward the edges. In contrast, Zone C exceeded 0.9 mm/m, which indicates localized subsidence and reduced serviceability.

Hydraulic performance evaluation demonstrated that the effective hydraulic conductivity in Zone B was $K_{eff} = 2.1 \times 10^{-4}$ m/s, with less than 10% deviation under cyclic loading up to 5000 cycles. The hydraulic stability coefficient (HSC = 0.93) confirmed sustained drainage capacity during rainfall events and elevated hydrostatic pressures. IoT-based moisture sensors further validated that the complete drainage time averaged 21.5 hours in Zone B, compared with more than 46 hours in Zone C, directly indicating reduced pore-pressure buildup in the reinforced section.

From an economic and environmental standpoint, the LCC/LCA analyses revealed that the traditional system, despite its lower initial cost (≈ 28 USD/m²), resulted in a cumulative 20-year cost of ≈ 52 USD/m². In contrast, the advanced system had a slightly higher initial cost (≈ 32 USD/m²) but limited the cost-growth rate and achieved a 20-year cumulative cost of ≈ 38 USD/m². The time-dependent cost model $C(t)=C_0 \times e^{\lambda t}$ yielded $\lambda = 0.024$ year^{-1} for the traditional method and $\lambda = 0.008$ year^{-1} for the geosynthetic-enhanced system, highlighting its long-term economic advantage.

The CO_2 emission assessment showed that the advanced system achieved an average annual reduction of $\Delta CO_2 \approx 1.8$ kg/m²/year, resulting in a total reduction of 36 kg/m² over 20 years and an overall decrease of approximately 30%.

This improvement was directly associated with reduced reconstruction frequency, optimized material sourcing, and the use of 3D-printed replacement components.

Compliance analysis with ASTM D4595, EN 13249, and ISO 10319 showed that Zone B exceeded the minimum required thresholds by 8–12% across all key mechanical indicators. The ultimate settlement performance also surpassed the European serviceability limit (≤ 20 mm) by more than a factor of two. This consistent enhancement emphasizes the practical significance of integrating advanced technologies into geotechnical infrastructure.

The Monte Carlo simulation with 10,000 iterations and a coefficient of variation of CV < 0.12 confirmed the statistical robustness of the results. Moreover, the correlation analysis between IoT sensor data and finite-element predictions yielded $R^2 = 0.86$ and RMSE = 0.092, demonstrating high predictive accuracy under complex loading conditions. Overall, the multi-layer interaction among geotextile, geogrid, and digital monitoring systems increased the operational performance index by approximately 1.38 times relative to the conventional system, reflecting a balanced improvement in mechanical, economic, and environmental metrics.

4. Conclusion

This study demonstrates that optimized integration of geosynthetic materials significantly enhances the mechanical, hydraulic, and environmental performance of infrastructure systems. Field measurements and numerical analyses across the three experimental zones (A, B, and C) confirmed that the geotextile–geogrid composite in Zone B achieved superior performance, with an average tensile strength of $\sigma_t = 41.2$ kN/m and an initial modulus of $E_i \approx 500$ kN/m. The final settlement in Zone B (9.8 mm) was reduced by more than 56% compared with the control zone (22.5 mm), while the settlement gradient remained below 0.35 mm/m, indicating improved deformation stability and more uniform stress distribution.

Micromechanical analysis revealed that the dual-reinforcement system enhanced particle interlocking and stress transfer between the granular and polymeric phases, resulting in a stiffer stress–strain response and a delayed onset of plastic deformation. IoT-based hydraulic monitoring further indicated that Zone B maintained an effective hydraulic conductivity of $K_{eff} = 2.1 \times 10^{-4}$ m/s and a hydraulic stability coefficient of HSC = 0.93 over 5000 loading cycles. The drainage time in Zone B was nearly twice as fast as in the traditional system (Zone C), confirming improved pore-pressure dissipation.

The LCA/LCC evaluation showed that the advanced system reduced the 20 year cumulative cost to ≈ 38 USD/m², compared with ≈ 52 USD/m² for the traditional method. Total CO_2 emissions also decreased from 118 to 82 kg/m², corresponding to an overall reduction of approximately 30% in alignment with SDGs 9 and 11. The decrease in annual cost growth rate (from $\lambda = 0.024$ to $\lambda = 0.008$ year^{-1}) validated the long term economic and environmental sustainability of the integrated system.

The measured indicators in Zone B exceeded the requirements of ASTM D4595, EN 13249, and ISO 10319 by 8–12%, while the statistical modeling ($R^2 = 0.86$, RMSE = 0.092) and the intraclass correlation

coefficient (ICC = 0.91) confirmed the accuracy and repeatability of the dataset.

Overall, the results highlight that integrating geosynthetics with modern monitoring technologies (BIM and IoT) not only enhances immediate mechanical–hydraulic performance but also extends structural service life, as reflected by the increased operational index (SI ≈ 1.38 × C-base). This study demonstrates that comprehensive geosynthetic systems offer a practical and effective approach for achieving high strength, hydraulic stability, and economic efficiency in modern infrastructure projects. Future work should focus on investigating the coupled thermo‑hydro‑mechanical (THM) behavior under environmental variations such as temperature, salinity, and moisture fluctuations, as well as developing data‑driven predictive models based on neural networks and metaheuristic algorithms to support next‑generation geosynthetic design.

5. References

[1] Firoozi, A.A. and Firoozi, A.A., 2023. Geotechnical solutions for urban centers: Bridging engineering innovations with socio-economic development. Sustain. *Soc. Dev*, *1*, pp.1-11. https://doi.org/10.54517/ssd.v1i3.2314

[2] Kuruşcu, A.O. and Girgin, Z.C., 2014. Efficiency of structural materials in sustainable design. *Journal of Civil Engineering and Architecture*, *October*, *8*(10), pp.1260-1265. https://doi.org/10.17265/1934-7359/2014.10.007

[3] Mengesha, G., 2025. Design Optimization in Structural Engineering: A Systematic Review of Computational Techniques and Real-World Applications. http://dx.doi.org/10.2139/ssrn.5254589

[4] Hasheminezhad, A., Ceylan, H., Kim, S. and Tutumluer, E., 2025. Geosynthetics for resilient geotechnics: A review of applications and innovations. *Transportation Geotechnics*, p.101676. https://doi.org/10.1016/j.trgeo.2025.101676

[5] Chatrabhuj and Meshram, K., 2024. Use of geosynthetic materials as soil reinforcement: an alternative eco-friendly construction material. *Discover Civil Engineering*, *1*(1), p.41. https://doi.org/10.1007/s44290-024-00050-6.

[6] Dąbrowska, J., Kiersnowska, A., Zięba, Z. and Trach, Y., 2023. Sustainability of geosynthetics-based solutions. *Environments*, *10*(4), p.64. https://doi.org/10.3390/environments10040064

[7] Markiewicz, A., Koda, E. and Kawalec, J., 2022. Geosynthetics for filtration and stabilisation: a review. *Polymers*, *14*(24), p.5492. https://doi.org/10.3390/polym14245492

[8] Heibaum, M., 2014. Geosynthetics for waterways and flood protection structures–Controlling the interaction of water and soil. *Geotextiles and Geomembranes*, *42*(4), pp.374-393. https://doi.org/10.1016/j.geotexmem.2014.06.003

[9] Shukla, S.K., 2025. *An introduction to geosynthetic engineering*. CRC Press.

[10] Singh, A. and Srivastava, A., 2025, October. Requirements and Applications of Geo-Composite in the Modern Civil Engineering Construction. *In Proceedings of the Indian Geotechnical Conference (IGC 2024), Volume 9: Geotechnical and Geophysical Investigation, Geomaterial Characterization, Site Investigation, and Exploration* (Vol. 9, p. 377). Springer Nature.

[11] Singh, S.K., Application of Geosynthetics in Civil Engineering Projects: Indian Scenario. *Guru Nanak Dev Engineering College Ludhiana (Punjab)-141006*, p.213.

[12] Antoljak, S., 2020, February. Geotechnical BIM in 2020. In *Geo-Congress 2020* (pp. 933-941). Reston, VA: American Society of Civil Engineers. https://doi.org/10.1061/9780784482810.097

[13] Ahmed, I.M. and Tsavdaridis, K.D., 2018. Life cycle assessment (LCA) and cost (LCC) studies of lightweight composite flooring systems. *Journal of Building Engineering*, *20*, pp.624-633. https://doi.org/10.1016/j.jobe.2018.09.013

[14] Shirazi, M.G., Rashid, A.S.A., Nazir, R.B., Rashid, A.H.A., Kassim, A. and Horpibulsuk, S., 2019. Investigation of tensile strength on alkaline treated and untreated kenaf geotextile under dry and wet conditions. *Geotextiles and Geomembranes*, *47*(4), pp.522-529. https://doi.org/10.1016/j.geotexmem.2019.01.016

[15] Attarchian, N., Tavakoli Mehrjardi, G., Zahaki, M. and Yousefi, A.A., 2025. Durability of non-woven geotextiles produced from recycled polyethylene terephthalate (PET). *Geosynthetics International*, *32*(4), pp.598-611. https://doi.org/10.1680/jgein.24.00077.

[16] Zanzinger, H. and Alexiew, D., 2022, October. Modified multiaxial tensile tests with geogrids in soil contact. In *IOP Conference Series: Materials Science and Engineering* (Vol. 1260, No. 1, p. 012030). IOP Publishing.

https://doi.org/10.1088/1757-899X/1260/1/012030.